Chemical reaction, Soret and Dufour impacts on Unsteady MHD Rotating fluid in a triangular duct

Dr.N.Vimala,Assistant professor(Adhoc),Department of Mathematics, Sri Krishna Devararya University College of Engineering & Technology, S.K.University,Anantapur-515003, India

Received: Aug 01, 2026 Accepted: Aug 28, 2026 Published: Aug 29, 2026

ABSTRACT

The control of the Newtonian heating on heat and mass transport in unsteady MHD flow of the fluid over the vertical plate with thermal radiation and chemical reaction has been explored in this current investigation. The fluid flow is induced due to periodic oscillations of the plate along its length and a uniform transverse magnetic field is applied in a direction which is normal to the direction of fluid flow. A Galerkin finite element method with linear triangular elements is used to obtain the global stiffness matrices. These coupled matrices are solved by an iterative scheme to obtain the solutions of the stream function, and the temperature and concentration fields. Also, the expressions for the stream function, and the temperature and concentration fields are obtained as a linear combination of the shape functions. The behaviours of the temperature field, the concentration field, the Nusselt number and the Sherwood number are discussed through graphs and tables for several sets of values of the governing parameters.

Key words: Chemical reaction, Soret effect, Dufour effect,MHD,Dissipation

1.Introduction.

The study of heat transfer and mixed convection flow in enclosures of various shapes has received attention due to its practical applications. Interest in these convection flow and heat transfer in porous medium has been motivated by a broad range of applications to geothermal systems, crude oil production, storage of nuclear waste materials, ground water pollution, fibre and granular insulations solidification of castings. In a wide range of such problems, the physical system can be modelled as a two-dimensional rectangular enclosure with vertical walls held at different temperatures and the connecting adiabatic horizontal walls. The stress that the two requirements for the occurrence of double-diffusive convection are that the fluid should contain two or more components with different molecular diffusivities and that these components make opposing contributions to the vertical density gradients.

The non-Newtonian fluids are mainly classified into three types, namely differential, rate, and integral. The simplest subclass of the rate type fluids is the Maxwell model which can predict the stress relaxation. This rheological model, also, excludes the complicated effects of shear dependent viscosity from any boundary layer analysis (Hayat et al. [1]). There is another type of non-Newtonian fluid known as Casson fluid. Casson fluid exhibits yield stress. It is well known that Casson fluid is a shear thinning liquid which is assumed to have an infinite viscosity at zero rate of shear, a yield stress below which no flow occurs, and a zero viscosity at an infinite rate of shear, i.e., if a shear stress less than the yield stress is applied to the fluid, it behaves like a solid, whereas if a shear stress greater than yield stress is applied, it starts to move. The examples of Casson fluid are of the type are as follows: jelly, tomato sauce, honey, soup, concentrated fruit juices, etc. Human blood can also be treated as Casson fluid. Due to the presence of several substances like, protein, fibrinogen, and globulin in aqueous base plasma, human red blood cells can form a chainlike structure, known as aggregates or rouleaux. If the rouleaux behave like a plastic solid, then there exists a yield stress that can be identified with the constant yield stress in Casson's fluid (Fung [2]). Casson fluid can be defined as a shear thinning liquid which is assumed to have an infinite viscosity at zero rate of shear, a yield stress below which no flow occurs, and a zero viscosity at an infinite rate of shear (Dash et al. [3]).Human blood may also be considered as Casson fluid owing to the presence of several substances they are, proteins, fibrinogens, globulins in aqueous base plasmas as well as human red blood cells. The mixed effects of mass and heat transfer with chemical reaction on the MHD (magnetohydrodynamic) flow of a viscous, incompressible, and electrically conducting fluid have attracted many researchers due to its wide range of engineering and industrial applications such as in MHD generators, plasma studies, nuclear reactors and geothermal energy extractions.Das et al. [4] studied the first order chemical reaction effect on the flow past an impulsively started infinite vertical plate with constant mass transfer and heat flux. Anjali Devi and Kandasamy [5] contemplated the mass and heat transfer on steady laminar flow along semi-infinite horizontal plate in the presence of chemical reaction. Andersson [6] studied the effect of magnetic field on the flow of a viscoelastic fluid past a stretching sheet. Nandkeolyar et al. [7] investigated the unsteady MHD heat and mass transfer flow of a heat radiating and chemically reactive fluid past a flat porous plate with ramped wall temperature.

Reddy et al. [8] presented a theoretical investigation of convective mass and heat transfer of unsteady MHD flow past a vertical semi-infinite porous plate with different viscosity and thermal conductivity. In recent years non-Newtonian fluids have outspread applications in chemical, pharmaceutical and cosmetic industries such as in the production of several chemicals, oil, gas, paint, syrup, juice, cleanser, and deodorizer [9]. In Newtonian fluid the viscous stresses arising from its flow, at every point are linearly proportional to the local strain rate and they have limited applications. They cannot describe various facts noticed for the fluids in industrial and other technological applications such as blood, soap, certain oils, paints, and many emulsions. It is well known that the mechanics of non-Newtonian fluids present a special challenge to engineers, physicists and mathematicians. Navier–Stokes' equations are not able to describe the properties of such fluids and no single constitutive equation is accessible which exhibits the properties of all fluids. Rheological properties of non-Newtonian fluids are described by their constitutive equations. Due to complex behavior of fluids, a number of non-Newtonian fluid models have been proposed such as viscoplastic [10], Bingham plastic [11], Brinkman type [12], power law [13], Oldroyd-B [14] andWalter-B [15] models.

on oblique stagnation point flow of a Casson-Nano fluid toward a stretching surface with heat transfer was presented by Nadeem et al. [16], and in the same year again Nadeem et al. [17] studied the MHD three dimensional boundary layer flow of Casson nanofluid past a linearly stretching sheet with convective boundary condition. In many realistic cases, the heat transfer from the surface is proportional to the local surface temperature. Such an effect is known as Newtonian heating effect. Merkin [18] investigated conjugate convective flow with Newtonian heating. Due to various applications researchers are attracted to consider the Newtonian heating condition in their problems. Hussanan et al. [19] presented an exact analysis of mass and heat transfer past a vertical plate with Newtonian heating. Recently, the unsteady boundary layer flowand heat transfer of a Casson fluid under the Newtonian heating boundary condition for non-Newtonian fluid was investigated by Hussanan et al. [20]. Das et al. [21] explored the Newtonian heating effect on unsteady MHD Casson fluid flow past a flat plate with heat and mass transfer. Ghosh and Mukhopadhyay [22] discussed the MHD slip flow and heat transfer of Casson nanofluid over an exponentially stretching permeable sheet. Khan et al. [23] investigated the comparative study of Casson fluid with homogeneous and heterogeneous reactions. Unsteady MHD free convection flow of Casson fluid past over an oscillating vertical plate embedded in a porous medium has been explored by Khalid et al. [24]. Rauf et al. [25] discussed the influence of convective conditions on three dimensional mixed convective MHD boundary layer flow of Casson nanofluid. Zaib et al. [26] explored the dual solutions of non-Newtonian Casson fluid flow and heat transfer over an exponentially permeable shrinking sheet with viscous dissipation. Raju et al. [27] discussed the heat and mass transfer in MHD Casson fluid over an exponentially permeable stretching surface.

2.Mathematical formulation of the problem

We consider the mixed convective heat and mass transfer flow of a viscous incompressible fluid in a saturated porous medium confined in the triangular duct (Figure 1) whose base length is a and height b. The heat flux on the base and top walls is maintained constant. The Cartesian coordinate system O(x, y) is chosen with origin on the central axis of the duct and its base parallel to the x-axis.

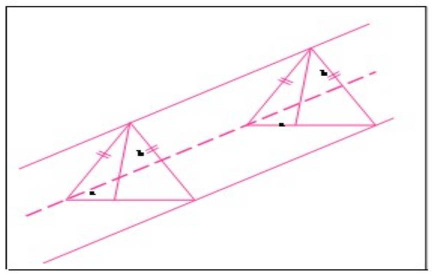

Figure I : Physical Configuration.

We assume that

i) The convective fluid and the porous medium are everywhere in local thermodynamic equilibrium.
ii) There is no phase change of the fluid in the medium.
iii) The properties of the fluid and of the porous medium are homogeneous and isotrophic.
iv) The porous medium is assumed to be closely packed so that Darcy's momentum law is adequate in the porous medium.
v) The Boussinesq approximation is applicable.

Under these assumption the governing equations are given by

$$\frac{\partial u'}{\partial x'}+\frac{\partial v'}{\partial y'}=0 \tag{1}$$

$$u'=-\frac{k}{\mu}\left(\frac{\partial p'}{\partial x'}\right) \tag{2}$$

$$v'=-\frac{k}{\mu}\left(\frac{\partial p'}{\partial y'}+\rho' g\right) \tag{3}$$

$$\left.\begin{aligned}\rho_\sigma c_p\left(u'\frac{\partial T'}{\partial x'}+v'\frac{\partial T'}{\partial y'}\right)=K_1\left(\frac{\partial^2 T'}{\partial x'^2}+\frac{\partial^2 T'}{\partial y'^2}\right)+Q(T_0-T)+\\ +\left(\frac{\mu}{K}\right)(u^2+v^2)-\frac{\partial(q_r)}{\partial x}\end{aligned}\right| \tag{4}$$

$$\rho_\sigma c_p\left(u'\frac{\partial C}{\partial x'}+v'\frac{\partial C}{\partial y'}\right)=D_1\left(\frac{\partial^2 C}{\partial x'^2}+\frac{\partial^2 C}{\partial y'^2}\right)-k'C \tag{5}$$

$$\rho'=\rho_0\left\{1-\beta(T'-T_0)-\beta^\bullet(C'-C_0)\right\} \tag{6}$$

$$T_0=\frac{T_h+T_c}{2},C_0=\frac{C_h+C_c}{2}$$

The appropriate boundary conditions are

$u' = v' = 0$ on the boundary of the duct
$T' = T_c$, $C = C_c$ on the side wall to the left
$T' = T_h$, $C = C_h$ on the side wall to the right

(7) $\frac{\partial T'}{\partial y} = 0$, $\frac{\partial C}{\partial y} = 0$ on the top ($y = 0$) and bottom

$u = v = 0$ walls ($y = 0$) which are insulated.

Invoking Rosseland approximation for radiation

$$q_r = \frac{4\sigma^*}{3\beta_R}\frac{\partial T'^4}{\partial y}.$$

Expanding T^4 in Taylor's series about T_e and neglecting higher order terms, we get

$$T'^4 \cong 4T_e^3 T - 3T_e^4.$$

We now introduce the following non-dimensional variables

$x' = ax$; $y' = by$; $c = b/a$
$u' = (\nu/a)\, u$; $v' = (\nu/a) v$; $p' = (\nu^2\rho/a^2)p$

$$T' = T_0 + \theta\,(T_h - T_c) \qquad C' = C_0 + \phi\,(T_h - T_c). \tag{8}$$

The governing equations in the non-dimensional form are

$$u = -\left(\frac{K}{a^2}\right)\frac{\partial p}{\partial x} \tag{9}$$

$$v = -\frac{k}{a^2}\frac{\partial p}{\partial y} - \frac{kag}{\nu^2} + \frac{kag\beta(T_h - T_c)\theta}{\nu^2} + \frac{kag\beta^\bullet(C_h - C_c)\phi}{\nu^2} \tag{10}$$

$$P\left(u\frac{\partial\theta}{\partial x} + v\frac{\partial\theta}{\partial y}\right) = \left(1 + \frac{4N}{3}\right)\left(\frac{\partial^2\theta}{\partial x^2} + \frac{\partial^2\theta}{\partial y^2}\right) - \alpha\theta + E_C\left(u^2 + v^2\right) \tag{11}$$

$$Sc\left(u\frac{\partial\phi}{\partial x} + v\frac{\partial\phi}{\partial y}\right) = \left(\frac{\partial^2\phi}{\partial x^2} + \frac{\partial^2\phi}{\partial y^2}\right) - k\phi \tag{12}$$

In view of the equation of continuity we introduce the stream function ψ as

$$u = \frac{\partial\psi}{\partial y}; \qquad v = -\frac{\partial\psi}{\partial x} \tag{13}$$

Eliminating p from the equation (9) and (10) and making use of (11) the equations in terms of ψ and θ are

$$\nabla^2\psi = -Ra\left(\frac{\partial\theta}{\partial x} + N\frac{\partial\phi}{\partial x}\right) \tag{14}$$

$$P\left(\frac{\partial\psi}{\partial y}\frac{\partial\theta}{\partial x} - \frac{\partial\psi}{\partial x}\frac{\partial\theta}{\partial y}\right) = \left(1 + \frac{4}{3N_1}\right)\left(\frac{\partial^2\theta}{\partial x^2} + \frac{\partial^2\theta}{\partial y^2}\right) - \alpha\theta \tag{15}$$

$$Sc\left(\frac{\partial\psi}{\partial y}\frac{\partial\phi}{\partial x} - \frac{\partial\psi}{\partial x}\frac{\partial\phi}{\partial y}\right) = \left(\frac{\partial^2\phi}{\partial x^2} + \frac{\partial^2\phi}{\partial y^2}\right) - k\phi \tag{16}$$

where

$G = \frac{g\beta(T_h - T_c)a^3}{\nu^2}$ (Grashof number)

$P = \mu c_p / K_1$ (Prandtl number)

$\alpha = Qa^2/K_1$ (heat source parameter)

$Ra = \frac{\beta g\left(T_g - T_c\right)Ka}{\nu^2}$ (Rayleigh number)

$N_1 = \frac{3\beta_R K_1}{4\sigma^\bullet : T_e^3}$ (radiation parameter)

$Sc = \dfrac{\nu}{D_1}$ (Schmidt number)

$N = \dfrac{\beta^*(C_h - C_c)}{\beta(T_h - T_c)}$ (buoyancy ratio)

$Ec = \left(\dfrac{a^4}{\mu K K_1 \Delta T}\right)$ (Eckert number) . $k = \dfrac{KL^2}{D_1}$ (chemical reaction parameter)

and the boundary conditions are

$$\frac{\partial \psi}{\partial x} = 0, \frac{\partial \psi}{\partial y} = 0 \text{ on } \quad x = 0 \text{ and } x = 1 \qquad (17)$$

$$\theta = 1 \quad \phi = 1 \quad \text{on} \quad x = 0, \text{ the side wall to the left}$$

$$\theta = 0 \quad \phi = 0 \quad \text{on} \quad x = 1, \text{ the side wall to the right.} \qquad (18)$$

3.Analysis of the numerical results

The control of the Newtonian heating on heat and mass transport in unsteady MHD flow of the Casson fluid over the vertical plate with thermal radiation and chemical reaction has been explored in this current investigation. The impact of governing variables on the flow domain is scrupulously inspected in the structure of graphically contours.

The Fig. 1 has been shown that, the fluid velocity slowed when the magnetic field parameter increasing to higher and higher levels. As the quantity of the magnetic field parameter increases, the layer thickness of the momentum boundary becomes thinner. The velocity graphics are characterized with a characteristic peak into the immediate region of the plate, and the magnetic field parameter boosted the decrease of those peaks while also causing a movement slowly downstream. It is because of the magnetic stripes of potency that are moving across the plate and the fluid that has its viscous forces lowered and received a push from the magnetic field, which worked to counteract the viscous results. This is the reason why it was successful. These findings are used in a wide variety of technical innovations.

The impact of penetrability parameter on velocity distribution is explored into the Fig. 2. Because of this, the velocity has increased due to a rising penetrability of porous medium. Therefore, a rise into the permeability of porous medium led to an increase in the flow of fluid while all of it is going on. The fluid velocity is demonstrated to be lower over the whole fluid expanse when the penetrability is reduced. These findings are also utilized in extracting petroleum as of crude oil, which falls within the purview of petroleum engineering.

The consequences of rotation on the final velocity are explored in the Fig. 3. It good known that the fluid component closest to the plate experiences an increase in its resultant velocity as the number of revolutions increases. The rotation improves the overall momentum achieved across the fluid area. Even though rotations are known to affect the velocity of fluid, the decelerating effects of these rotations are only seen into the fluid medium near to the plate, where they have the opposite effect on the remaining region, and eventually, they disappear altogether. This is a direct consequence of the observation that the Coriolis forces predominate in area near an axis of rotation.

Figures 4and 5 depicted the impacts of the thermal Grashof number Gr and the mass Grashof number Gm on the velocity distribution. A rise in the thermal Grashof number Gr and the mass Grashof number Gm contributes to a corresponding increase in the velocity magnitude. Because buoyancy forces operate on the fluid particles in a way that is compatible with gravitational forces, the momentum of the fluid is increased. This tendency may be explained by the fact that the positive Grashof number Gr functioning in a manner analogous to the advantageous pressure gradient; these go faster the fluids to the border layer. Since a direct consequence, there is a rise in Gr,which led to an increase in velocity. Thermal Grashof number reflects the impacts of freed convective currents. $Gr > 0$ denotes the temperature of the fluid of cooling of the boundary surface, $Gr < 0$ indicates the cool of the fluid of the temperature of the boundary surface, and $Gr = 0$ corresponds to the lack of free convective currents. These conclusions are also utilized to study heat and mass transfer in industrial, mechanical, and aeronautical engineering, respectively.

The velocity patterns at different Casson parameter values are presented in the Fig. 6. Since the higher values of the Casson parameter, then the lower the yield stresses and the more the velocity field is dampened. When the Casson parameter value is exceedingly significant, the fluid exhibits the characteristics of a Newtonian fluid. The observation that higher quantities of the Casson parameter results into lower velocity is subject to investigation. As a result, using Fig. 7 as a reference, one may deduce that the velocity contours for dissimilar quantities of the Newtonian heating parameter exist. The velocity field is slow down as the quantities of the heating parameter in the Newtonian model increased. The fact that the velocity reduces as the values of the Newtonian heating parameter augment is being investigated.The Fig. 8 shows the velocity distribution for the different values of time. It can be deduced from the figure that, the velocity also rises as the quantities of the non-dimensional time enlarges.The temperature distribution is designed and is shown in the Figs. 9, 10, 11, 12 together with the thermal radiation parameter Nr, the Prandtl number Pr, and the non-dimensional time. It may be explored from the Figs. 9, 10 that, the temperature delivery rises when the thermal radiation parameter and the Newtonian heating parameter are both increased. The reduction in the temperature distribution owing to an amplifying in the Prandtl number is seen in Fig. 11. This happens because a reduced velocity would imply that it does not converse rapidly, so that the surface temperature would decrease. It has been investigated and shown that the temperatures distribution rises along by an augment in the non-dimensional time parameter (Fig. 12).The concentration distribution for the pertinent parameters, which are including the Schmidt number Sc, the chemical reaction parameter Kc, and the non-dimensional time parameter, and are explored in the Figs. 13, 14, 15. This can be demonstrated from the Figs. 13, 14 that, an amplifying in the Schmidt numbers Sc results in a decrease in the concentration field. An ever-increasing chemically reactive parameter called Kc is also used to evaluate the performance of an equivalent system. The primary reason for this is that the number of solvent molecules undergoing chemical reaction increase as the number of responding parameters rises; hence, the concentration field sees a decline due to this phenomenon. The area of chemical engineering also uses this idea to create mixtures of nanofluids. Last but not least, it is discovered that the concentration distribution expands with an augment in the non-dimensional time parameter (Fig. 15).

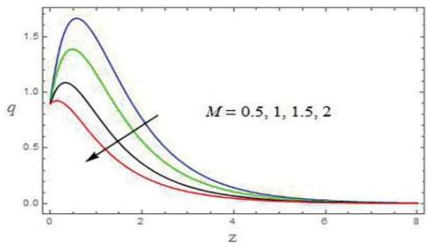

Fig.1. The Velocity Profiles against M

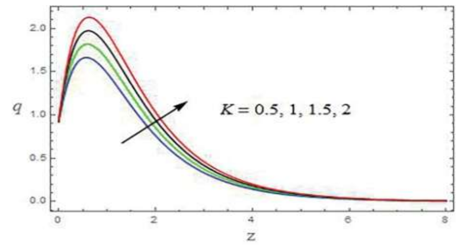

Fig.2. The Velocity Profiles against K

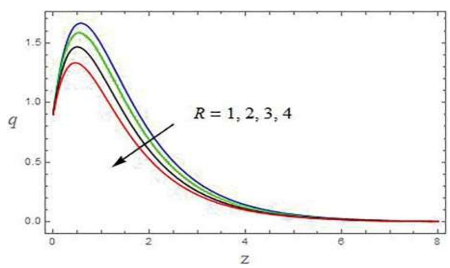

Fig.3 The Velocity Profiles against R

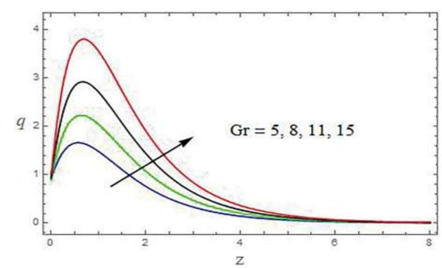

Fig.4.The Velocity Profiles against Gr

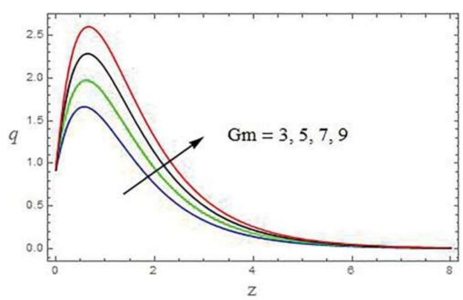

Fig.5. The Velocity Profiles against Gm

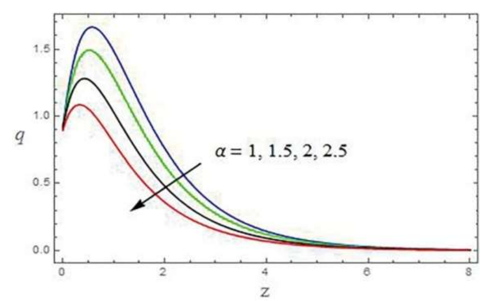

Fig.6. The Velocity Profiles against α

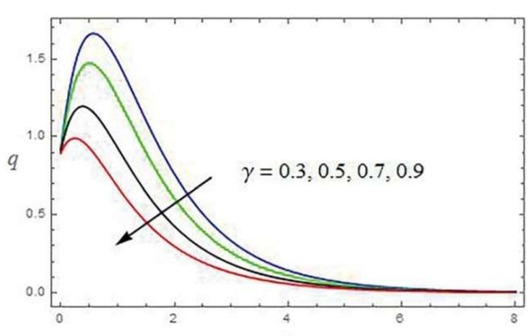

Fig.7. The Velolcity Profiles against γ

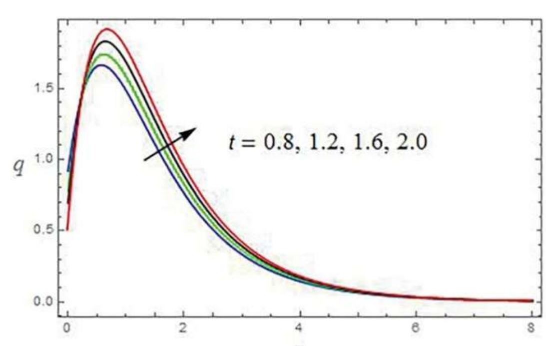

Fig.8. The Velocity Profiles against t

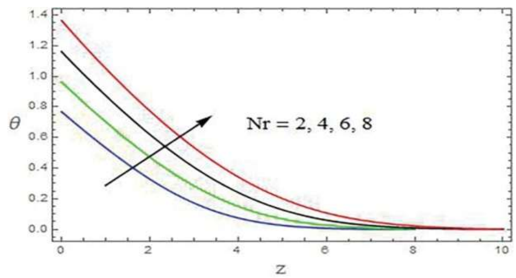

Fig,9 The Temperature Profiles against Nr

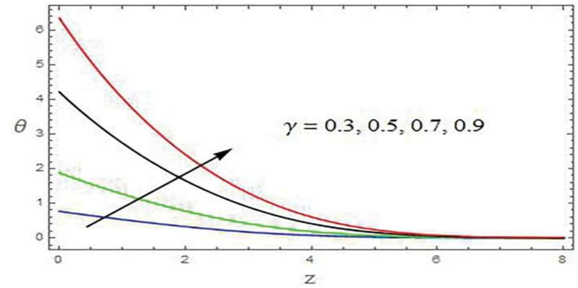

Fig.10. The Temeperature Profiles against γ

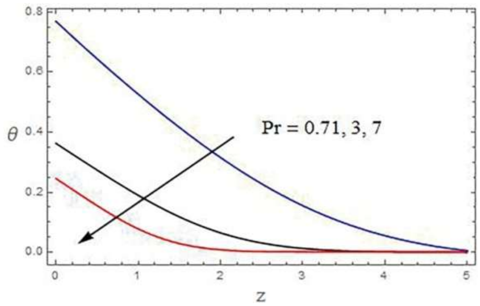

Fig.11. The Temperature Profiles against Pr

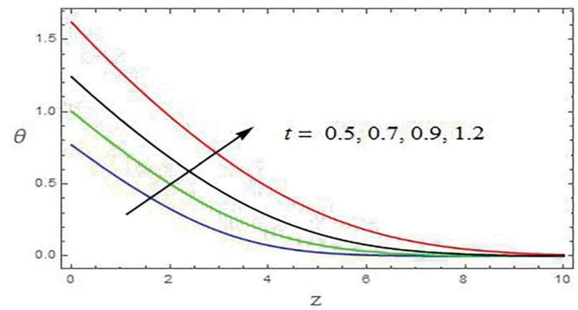

Fig.12. The Temperature Profiles against t

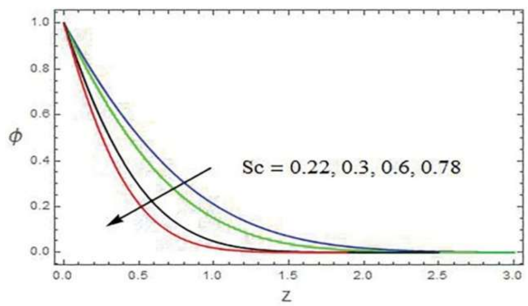

Fig.13. The Temperature Profiles against Sc

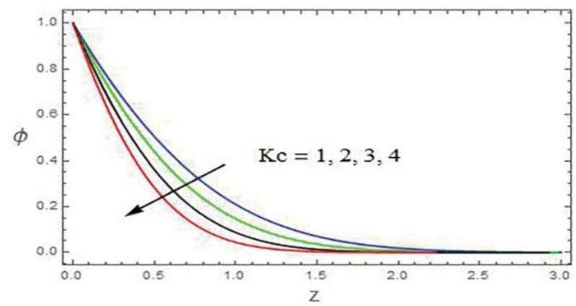

Fig.14.The Temperature Profiles against Kc

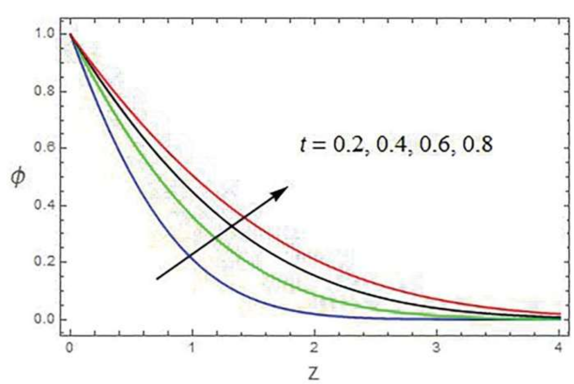

Fig.15. The Temperature Profiles against t

Table.1.Skin friction

M	K	R	Gr	Gm	α	γ	t	τ
0.5	0.5	1	5	3	1.0	0.3	0.8	0.979726
1								1.166616
1.5								1.368948
	1.0							0.783235
	1.5							0.575839
		2						1.139839
		3						1.331798
			8					0.796135
			11					0.568838
				5				0.768905
				7				0.545666
					1.5			1.37884
					2.0			1.782837
								0.812837
								0.584829
								0.902205
								0.769147
						0.5		1.145825
						0.7		1.366909
							1.2	0.886507
							1.6	0.775505

Table.2.Nusselet number

Nr	γ	Pr	t	Nu
2	0.3	0.71	0.5	1.183930146
4				0.969795656
8				0.856863441
	0.5			1.245770145
	0.7			1.319810015
		3.0		2.196380123
		7.0		3.240170333
			0.7	0.906123001
			0.9	0.784768148

Table.3. Sherwood number

Sc	Kc	*t*	Sh
0.22	1	0.2	2.295710025
0.30			2.658221254
0.60			3.703509966
0.78			4.203750021
	2		2.375114156
	3		2.466613326
	4		2.56708664
		0.4	1.718911237
		0.6	1.481039986
		0.8	1.350896523

Tables 1, 2, 3 for the skin friction, rate of heat transport, and rate of mass transport, together with the corresponding values of the governing parameters have been developed. This may be explored from Table 1 ththe rotation parameter R, the Casson fluid parameter, and the Newtonian heating parameter all amplify the skin friction. In contrast, an enlargement in the permeability parameter K, and the thermal Grashof number Gr correspondingly slowly it down. It is also said that, the rate of heat transport increase when there is an augment in the heat source parameter S and the time t; however, the rate decreases when there is an increase in the Prandtl number Pr(Table 2). In Table 3, the influence of Schmidt numbers Sc, the chemical reaction parameter Kc, and time t on Sherwood number are represented and illustrated. It has been discovered that, the rate of mass transport quicken with an increase in the Schmidt number Sc or the chemical reaction parameter Kc. Still, it is slowly down with the rise in the time t.at, an augment in the Hartmann number M.

4. References

[1] Hayat, T., Awais,M., Sajid,M.: Mass transfer effects on the unsteady flow of UCM fluid over a stretching sheet. Int. J. Mod. Phys. B 25, 2863–2878 (2011)
[2].Fung, Y.C.: Biodynamics: circulation. Springer, New York (1984). https://doi.org/10.1007/978-1-4757-3884-1
[3]. Dash, R.K., Mehta, K.N., Jayaraman, G.: Casson fluid flow in a pipe filled with a homogeneous porous medium. Int. J. Eng. Sci. 34(10), 1145–1156 (1996)
[4]. Das, U.N., Deka, R., Soundalgekar, V.M.: Effects of mass transfer on flow past an impulsively started infinite vertical plate with constant heat flux and chemical reaction. Forschung im Ingenieurwesen-Eng.Res. 60, 284–287 (1994)
[5]. Anjalidevi, S.P., Kandasamy, R.: Effects of chemical reaction, heat and mass transfer on laminar flow along a semi infinite horizontal plate. Heat Mass Transf. 35(6), 465–467 (1999). https://doi.org/10.1007/s002310050349
[6]. Andersson, H.I.: An exact solution of the Navier Stokes' equations for magnetohydrodynamic flow. Acta Mech. 113, 241–244 (1995)
[7]. Nandkeolyar, R., Das, M., Sibanda, P.: Unsteady hydromagnetic heat and mass transfer flow of a heat radiating and chemically reactive fluid past a flat porous plate with ramped wall temperature.Math. Probl.Eng. 2013, 1–6 (2013)
[8]. Reddy, M.G., Reddy, N.B., Reddy, B.R.: Unsteady MHD convective heat and mass transfer flow past a semi infinite vertical porous plate with variable viscosity and thermal conductivity. Int. J. Appl. Math.Mech. 5(6), 1–14 (2009)
[9]. Chaoyang,W., Chuanjing, T.U.: Boundary-layer flow and heat transfer of non-Newtonian fluids in porous media. Int. J. Heat Fluid Flow 10(2), 160–165 (1989)
[10]. Hassan, M., Pathak, M., Khan, M.K.: Natural convection of viscoplastic fluids in a square enclosure. J.Heat Transf. 135(12), 122501 (2013)
[11]. Kleppe, J., Marner, W.J.: Transient free convection in a bingham plastic on a vertical flat plate. J. Heat Transf. 94(4), 371–376 (1972)
[12]. Zakaria, M.N., Hussanan, A., Khan, I., Shafie, S.: The effects of radiation on free convection flow with ramped wall temperature in Brinkman type fluid. J. Teknol. 62(3), 33–39 (2013)
[13]. Olajuwon, B.: Flow and natural convection heat transfer in a power law fluid past a vertical plate with heat generation. Int. J. Nonlinear Sci. 7(1), 50–56 (2009)
[14]. Khan, I., Fakhar, K., Anwar, M.I.: Hydromagnetic rotating flows of an Oldroyd-B fluid in a porous medium. Special Top. Rev. Porous Media 3(1), 89–95 (2012)
[15]. Khan, I., Farhad, A., Sharidan, S., Qasim, M.: Unsteady free convection flow in aWalter-B fluid and heat transfer analysis. Bull. Malay. Math. Sc. Soc. 37, 437–448 (2014)
[16]. Nadeem, S., Mehmood, R., Akbar, N.S.: Oblique stagnation point flow of a Casson-nano fluid towards a stretching surface with heat transfer. J. Comput. Theor. Nanosci. 11(6), 1422–1432 (2014)
[17]. Nadeem, S., Haq, R.U., Akbar, N.S.: MHD three-dimensional boundary layer flow of Casson nanofluid past a linearly stretching sheet with convective boundary condition. IEEE Trans. Nanotechnol. 13(1),109–115 (2014)
[18]. Merkin, J.H.: Natural-convection boundary-layer flow on a vertical surface with Newtonian heating. Int.J. Heat Fluid Flow 15(5), 392–398 (1994)
[19]. Hussanan, A., Khan, I., Shafie, S.: An exact analysis of heat and mass transfer past a vertical plate with Newtonian heating. J. Appl. Math. 2013(1), 4345719 (2013)
[20]. Hussanan, A., Salleh, M.Z., Tahar, R.M., Khan, I.: Unsteady boundary layer flow and heat transfer of a Casson fluid past an oscillating vertical plate with Newtonian heating. PLoS ONE 9(10), e108763 (2014)

[21]. Das, M., Mahato, R., Nandkeolyar, R.: Newtonian heating effect on unsteady hydro-magnetic Casson fluid flow past a flat plate with heat and mass transfer. Alex. Eng. J. 54(4), 871–879 (2015)

[22]. Ghosh, S., Mukhopadhyay, S.:MHDslip flow and heat transfer of Casson nanofluid over an exponentially stretching permeable sheet. Int. J. Auto. Mech. Eng. 14(4), 4785–4804 (2017)

[23]. Khan, M.I., Waqas, M., Hayat, T., Alsaedi, A.: A comparative study of Casson fluid with homogeneousheterogeneous reactions. J. Colloid Interface Sci. 498, 85–90 (2017)

[24]. Khalid, A., Khan, I., Khan, A., Shafie, S.: Unsteady MHD free convection flow of Casson fluid past over an oscillating vertical plate embedded in a porous medium. Eng. Sci. Technol. Int J. 18, 309–317 (2015)

[25]. Rauf, A., et al.: Influence of convective conditions on three dimensional mixed convective hydromagnetic boundary layer flow of Casson nanofluid. J. Magn. Magn. Mater. 416, 200–207 (2016)

[26]. Zaib, A., Bhattacharyya, K., Uddin, M., Shafie, S.: Dual solutions of non-Newtonian Casson fluid flow and heat transfer over an exponentially permeable shrinking sheet with viscous dissipation. Model. Simul.Eng. 2016, 1–8 (2016). https://doi.org/10.1155/2016/6968371

[27]. Raju, C.S.K., Sandeep, N., Sugunamma, V., Babu, M.J., Reddy, J.R.: Heat and mass transfer in magnetohydrodynamic Casson fluid over an exponentially permeable stretching surface. Eng. Sci. Technol. Int J. 19, 45–52 (2016)